

CONSIDERATIONS REGARDING THE ALIGNMENT OF DIFFRACTOMETERS FOR RESIDUAL STRESS ANALYSIS

THOMAS R. WATKINS¹, O. BURL CAVIN², CAMDEN R. HUBBARD¹, BETH MATLOCK³, AND
ROGER D. ENGLAND⁴

¹ *Metals Materials Science & Ceramics Technology Division, Oak Ridge National Laboratory, Oak Ridge, TN 37831-6064, U.S.A.*

² *Center for Materials Processing, University of Tennessee, Knoxville, TN 37996-0750, U.S.A.*

³ *TEC/Materials Testing Division, 10737 Lexington Drive, Knoxville, TN 37932, U.S.A.*

⁴ *Cummins Inc., Columbus, IN 47201, U.S.A.*

Proper alignment of an X-ray diffractometer is critical to performing credible measurements, particularly for residual stress determinations. This article will emphasize practical aspects of diffractometer alignment and standards usage with regards to residual strain measurement. Essentially, what to do when one is confronted with a residual stress problem and an unfamiliar goniometer. Various alignment techniques, use of standards, and related issues will be discussed.

1. Introduction

An important and often overlooked aspect of diffraction work is proper diffractometer alignment. Residual stress determinations require a well-aligned goniometer, particularly with focusing or Bragg-Brentano optics. A well-aligned goniometer means that the X-ray source, goniometer center and back slit are all co-planar and that the ability to reproducibly place the sample surface on the goniometer's center of rotation has been demonstrated. The use of new parallel beam optics (PBO) such as multi-layer parabolic mirrors or polycapillary optics for residual stress measurements is preferred since PBO can reduce or eliminate peak shifts due to sample displacement, specimen transparency, and flat specimen errors. Though parallel beam optics may have relaxed the alignment rigor necessary to do residual stress determinations, it is still vital for the practitioner to know where the beam is going in order to have confidence in data interpretation [1].

The subject of this paper is not new, and the cited references are not exhaustive. Also, it should be noted that depending upon the equipment involved, the outlined steps may vary. Rather than an extensive discussion of alignment found elsewhere [2, 3], the objective here is to emphasize "down-and-dirty" practical usage and techniques necessary to safely align a typical powder diffractometer for a residual stress determination. That is, essentially, what one does when confronted with a new machine to ensure it is running properly, how to use

standards in this effort, what are the related errors and practical examples. This paper evolved, in part, out of portions of workshops given at the Denver X-ray Conference [4, 5]. After a brief discussion of safety, this paper seeks to answer four questions:

1. How to know when the alignment is good enough? (What do I want to do with this instrument?)
2. How to check the alignment of a goniometer? (What tests do I perform?)
3. How to improve the alignment of a goniometer? (What should I change?)
4. How do I maintain the alignment?

In order to clearly illustrate these tests, real data will be discussed from a 4-circle/axis system [6] that has just had the tube changed from Co to Cu and a 2-circle/axis system that was due for an alignment check (see Fig. A1 in Appendix A[#]). Appendix A provides details about the instruments and data collection. Since the base configuration of the 4-axis system is basically that of a θ - 2θ system, this unit will also be referred to as either the 4-axis or θ - 2θ system, depending on the nature of the testing being discussed.

2. Safety

The greatest likelihood of a personal X-ray exposure is during alignment. Today, live-beam alignment, while quick, is no longer considered

[#] Appendices available at www.rigakumsc.com/journal/index.jsp

Table I. Elements of testing the fail-safe or interlock circuit of an X-ray diffractometer.

Question: What happens if the enclosure door is opened when the generator is energized and the shutter is open?

1. Obtain fail-safe circuit and performance description from manufacturer
2. Sequence and conduct testing in safe manner
3. Restrict admittance to lab during testing
4. Avoid live beam
5. Generator is ON and shutter is OPEN
6. Open or attempt to open enclosure door...what happens? Does the shutter close? Does the generator de-energize? Nothing?
7. Now close enclosure door...what happens? Does the system self-actuate (close and play)?

Question: What happens if either the "Generator On" or "Shutter Open" indicator light burns out? [Simulate by removing light bulb]

- 1.-4. As above
5. While generator is energized, *safely* remove the "Generator On" light bulb...what happens? Does the generator de-energize? Nothing?
6. While generator is OFF, remove the "Generator On" light bulb...Will the generator now start?
7. With shutter *closed* and the generator energized, remove "Shutter Open" indicator bulb...what happens?
8. Next, close enclosure door and attempt to open shutter...what happens?

Questions: Based on the above, does circuit perform as advertised? Are you "happy" or concerned? Consult manufacturer and make modifications if needed.

a safe option; thus, a slower, safer, incremental alignment methodology is utilized. Still care and caution must be exercised. Since the custodian is in and out of the X-ray enclosure/hutch frequently making small adjustments to the system, he/she must be vigilant as to the status of the shutter. It is understood in the following discussion that any changes made by the custodian inside the X-ray enclosure/hutch are done so with the shutter closed.

There are other points to consider. The fail-safe circuit with a clear performance description should be obtained from manufacturer, which needs to be understood and tested periodically (see Table I). The custodian should obtain and use a survey meter/Geiger counter for laboratory use to check for leaks around tube heads and more general surveys. In particular, if the target/X-ray tube is changed from a longer to shorter wavelength (viz. lower to higher energy), a radiological survey should be conducted at full power with the shutter closed around the tube head and again with the enclosure closed and the shutter open to check for leaks and/or inadequate shielding. The material from which the shutter is made needs to be determined. In the past, lead was commonly used for shutter material. Unfortunately, time and experience have shown that lead is a particularly poor shutter material, as lead shutters are known to stick, jam or freeze open or closed [7]. X-rays produce ozone in an ambient atmos-

phere [8], and ozone is very corrosive, particularly in humid atmospheres [9]. The lead corrodes, likely due to the ozone, forming a *sticky* grayish white corrosion product. Empirical observation has revealed that shutter assembly components made of Ni-coated brass also corrode. In the past and with less intense X-ray sources, the user simply cleaned the shutter frequently to alleviate the problem. Today, there are better solutions available. If your shutter contains lead, it should be replaced with a sufficiently thick piece of tantalum or 304L stainless steel (perhaps lead filled). Periodic inspections of the shutter are still recommended. Mechanical binding or solenoid failure can also cause the shutter to jam open or closed. Again, lead is a soft and malleable metal, which can deform/wear over time to cause a jam. A secondary safety circuit is often desirable [7, 10]. Finally, one should *never* rely solely on the software to determine the status of the shutter.

3. How to know when the alignment is good enough? (What do I want to do with this instrument?)

While well-aligned and well maintained instruments are necessary to do any good work, it is important to know just how "good" the alignment needs to be for the task at hand, given the time and financial constraints we all face. Table II lists some general guidelines or "rules of thumb" when checking the alignment regarding

Table II. General guidelines or “rules of thumb” regarding alignment using a standard/reference powder.

The alignment is good enough for <i>Blank 1</i> when the peak positions <i>Blank 2</i>	
<i>Blank 1</i>	<i>Blank 2</i>
Phase identification	of strong reflections locate within $<0.05^\circ$ of reference pattern for 10 to $45^\circ 2\theta$.
Pole figure	locate within $\sim 0.2^\circ$ of reference pattern for 10 to $45^\circ 2\theta$.
Stress	locate within 0.03° of reference pattern for $\geq 130^\circ 2\theta$ and the reference powder peak position shift with tilting is $\leq 0.03^\circ$ for the entire ψ range.
Precision lattice parameters	locate within $\sim 0.01^\circ$ for 10 to $160^\circ 2\theta$.
The alignment is good enough for <i>Blank 3</i> when the peak resolution <i>Blank 4</i>	
<i>Blank 3</i>	<i>Blank 4</i>
Phase identification, Stress or Precision lattice parameters	has a figure of merit (FOM) for the five fingers of quartz >2 . ²
Pole figure	or FWHM $\sim 0.2^\circ$ for 10 to $45^\circ 2\theta$.

peak position and resolution with a standard/reference material, preferably a powder of -325 mesh/ $<45 \mu\text{m}$ particle size. For residual stress determinations, the relative differences in peak position are more important than the absolute position. As always, sample knowledge (composition, etc.) and good software help immensely.

Peak resolution here refers to the relationship between peak width or full width at half maximum (FWHM) with respect to peak overlap. That is, for a given FWHM, the resolution is defined by how close can two peaks overlap before they are indistinguishable and resemble a single broadened peak. Today there are often many choices of optics all of which have certain advantages and disadvantages relative to each other. Generally for a given diffractometer system, improving the resolution results in the reduction of the intensity of the peaks, which can significantly increase the data collection time, particularly in the high two theta region where data for stress determinations are acquired and where peaks are inherently much weaker. While high resolution may be required when working with multiphase samples and/or low symmetry phases, most stress determinations are performed on predominantly single-phase engineering materials, which generally have high symmetry crystallographic structures, and thus do not require high resolution.

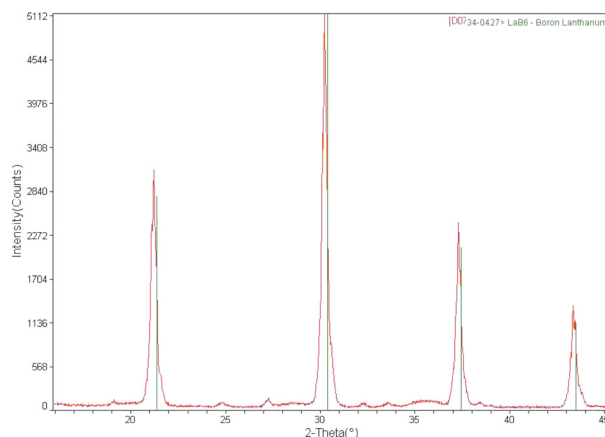


Fig. 1. 4-axis unit: Diffraction pattern of LaB_6 shows peak positions are systematically low at low 2θ (see full pattern in Fig. B1) relative to PDF card #34-427.

4. How to check the alignment of a goniometer? (What tests do I perform?)

First, the custodian collects a set of diffraction data covering a wide 2θ angle (see Appendix B for details). This involves collecting a diffraction pattern from a standard/reference powder or stress-free sample via a θ - 2θ scan. The peak positions and calculated lattice parameters are compared relative to the standard values in a database and prior instrument records. Fig. 1 shows a portion of a LaB_6 diffraction pattern taken on the 4-axis unit, wherein the low 2θ peak positions are low relative to the PDF card #34-427 [11]. The refined lattice parameter determined from this scan was 4.1598(4) as com-

pared to the PDF value of 4.15690 Å (see Table BI). Likewise, the data in Fig. 2 from the θ - θ unit shows LaB₆ peak positions are systematically high in the high 2 θ region with a refined lattice parameter of 4.1518(2) Å (see Table BII). It is obvious that some re-alignment is needed on both instruments.

Next the custodian conducts intensity, FWHM/resolution and X-ray wavelength contamination tests (see Appendix C for details). This involves collecting a diffraction pattern from a polycrystalline quartz plate via a θ -2 θ scan over selected 2 θ regions. Fig. 3 indicates that the detector electronics and diffraction side monochromator are set properly as no $k\beta$ peak is observed. Further, the tube potentially has a lot of

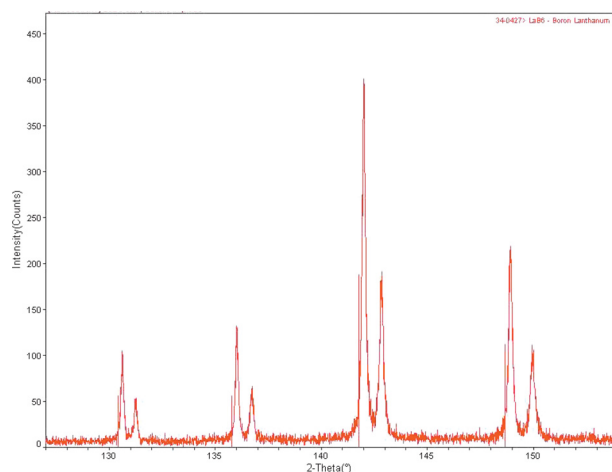


Fig. 2. θ - θ unit: Diffraction pattern of LaB₆ shows peak positions are systematically high at high 2 θ (see full pattern in Fig. B2) relative to PDF card # 34-427.

life left given the high intensity and negligible $W_{L\alpha}$ lines caused by target contamination. The intensity test was not done on the 4-axis unit as a brand new tube was installed. The five fingers of quartz were examined using both instruments, wherein the $k_{\alpha_1-\alpha_2}$ of three reflections overlap in such a way as to resemble the fingers of a hand. A figure of merit (FOM) is calculated from the intensity of the (212) minus the background intensity divided by the average intensity of the valleys surrounding the (212) line [i.e., trough between (212) _{$\alpha_1-\alpha_2'$} , (212) _{α_2} -(203) _{α_1'} , (301) _{$\alpha_1-\alpha_2$}] minus the background intensity. Generally, an acceptable performance the FOM should be greater than 2. The test result for the 4-axis unit was particularly bad (see Fig. 4) and resembled a mitten. This poor resolution is due to the 0.25° radial divergence limiting (RDL) slits on the diffraction side. These RDL slits present a tradeoff: reduced sensitivity to sample surface displacement and in this case enhanced intensity versus resolution. As was pointed out above, good resolution is often not needed for residual stress determinations and texture studies. In contrast, the FOM from the θ - θ is good, exceeding 2 (see Fig. 5). Although not critical to residual stress determinations, Appendix D covers how to handle dead time corrections for detectors.

The “tilt” test [12] quickly checks for X-ray beam misalignment and/or sample surface displacement (with Bragg-Brentano optics), which is required prior to residual stress determinations. If parallel beam optics (PBO) are used, the confounding influence of slight sample surface

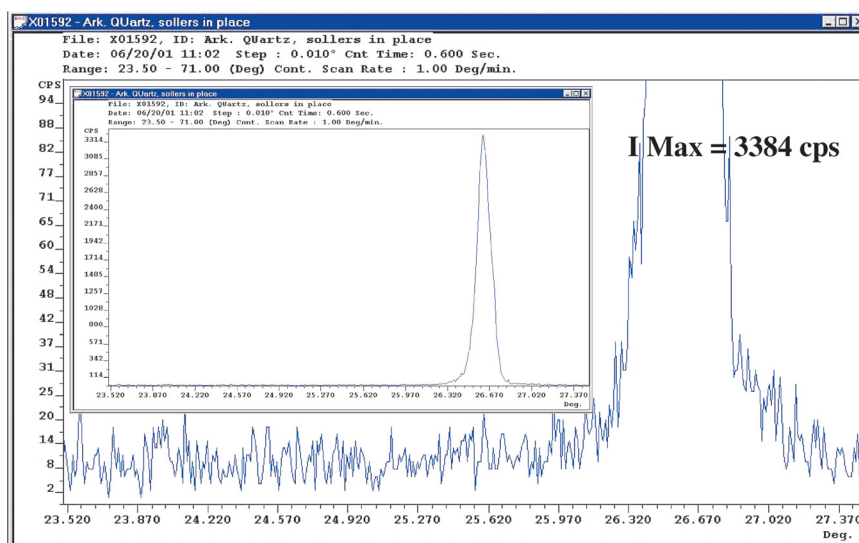


Fig. 3. θ - θ unit: Diffraction pattern of Quartz shows no $k\beta$ and negligible W contamination. Inset: good peak intensity for (101) reflection of quartz.

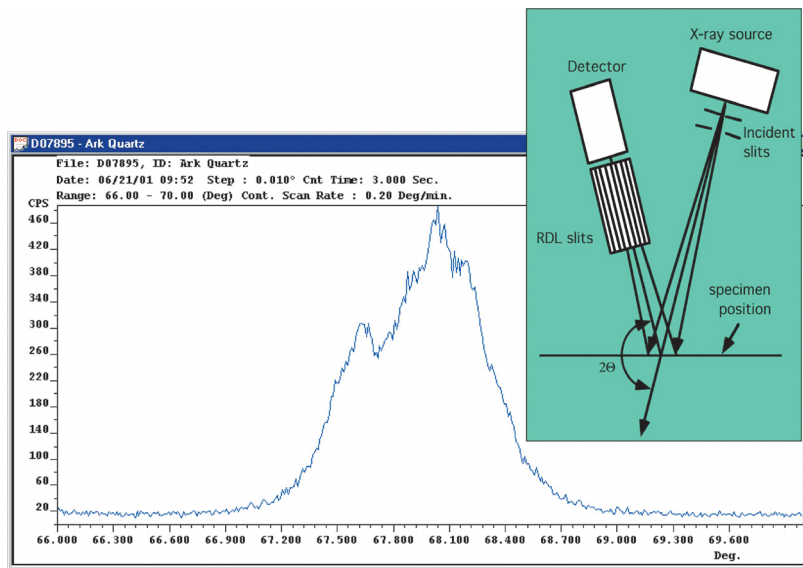


Fig. 4. 4-axis unit: The “mitten” of Quartz. Inset shows a schematic representation of the optics. Not shown: incident Soller slits.

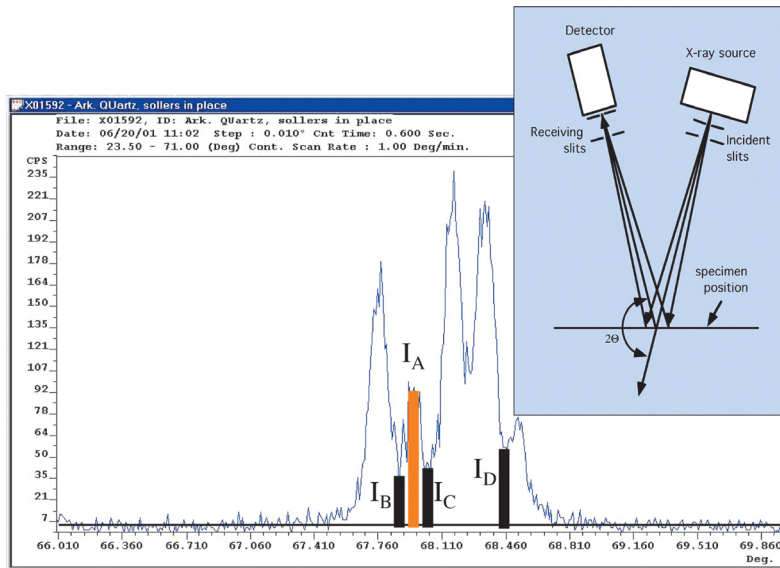


Fig. 5. Θ - Θ unit: The five fingers of quartz, $FOM=3I_A/(I_B+I_C+I_D)=2.29$. Inset shows a schematic representation of the optics. Not shown: incident and receiving Soller slits and diffraction side monochromator.

displacement is removed. Here, a strain/stress-free sample, usually a powder, is mounted on the goniometer and tilted the same as in a stress determination. If the goniometer is aligned and the sample surface is on the center of rotation of the goniometer, the amount of peak shift will be very small. A LaB_6 powder sample was slurry-mounted on a zero background plate. This sample was placed on the 4-axis unit, which has both χ and Ω axis movements (the goniometer movements are shown in Figs. A2 and A3, respectively, wherein $\chi=\Psi$

and $\Omega=2\theta/2\pm\Psi$). The sample was oscillated to improve particle statistics; if available, oscillation is recommended as it improves peak shape. The (510) reflection was examined at $\sim 141.8^\circ 2\theta$ with only three Ψ tilts (more may be required/desired as in a stress determination). Tilt tests should include both positive and negative Ψ tilts covering as large an angular range as possible. The results for each are shown in Figs. 6 and 7, respectively, all of which show very small relative peak shifts despite an error in absolute peak position relative to the PDF

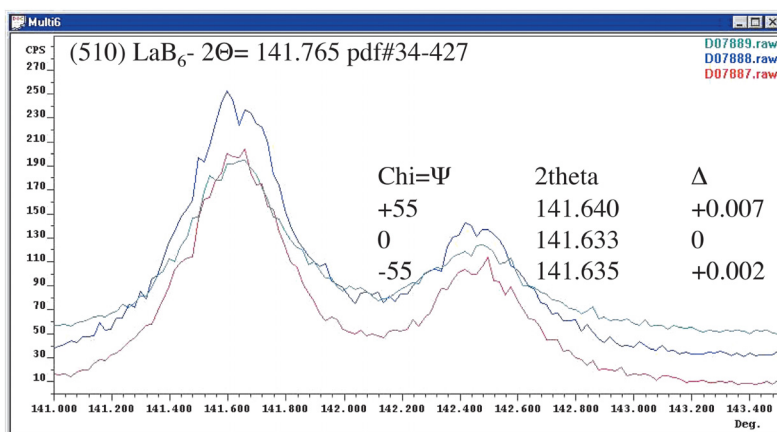


Fig. 6. 4-axis unit: Tilt test using chi axis shows acceptable tilting alignment.

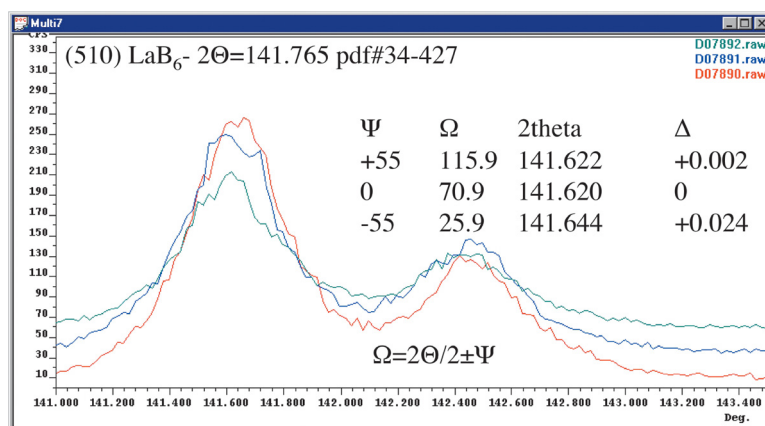


Fig. 7. 4-axis unit: Tilt test using omega axis shows acceptable tilting alignment.

card.

5. How to improve the alignment of a goniometer? (What should I change?)

The generic step-by-step re-alignment of a 4-axis and θ - θ goniometers will be described in three broad overlapping steps: goniometer inspection, 4 "physical" alignment (no diffraction) and diffraction alignment. Since the custodian typically has little or no recourse, misalignment of goniometer axes relative to each other or relative to the position to the center of rotation will be assumed to be negligible and not discussed. Prior to beginning alignment for the first time, the custodian should inspect his goniometer and construct a functional schematic drawing of his goniometer (see Fig. 8), which shows all the parts that can be adjusted or moved relative to the others. Usually there is one spot on the goniometer/beam path which cannot be moved or which the custodian has only limited control over its position, such as the center of rotation on the goniometer (as is the case for both ex-

amples here) or the focal spot, respectively. These become important as it usually defines the sequence of the alignment.

The physical alignment involves leveling, physical settings and using the X-ray beam without doing any diffraction. The following are handy alignment tools to have: fluorescent screen, dial indicator, mounting hardware and pin, sample situated alignment pieces (e.g., "glass slit," knife edge(s), flat plate), reference powders and materials, attenuating foils, level, "X-ray sensitive burn paper," telescope/cathetometer, direct beam detector, and other tools specially fabricated for you. A good deal of patience and courage is also needed.

First, level the goniometer. This may be accomplished by pre-existing adjustment screws or may require shims. Confirm or adjust the take off angle from the focal spot, which is typically, but not always, 6° (purple arc in Fig. 9). Alignment should always be performed at the normal power settings you intend to use to collect data, as the focal spot generally will move

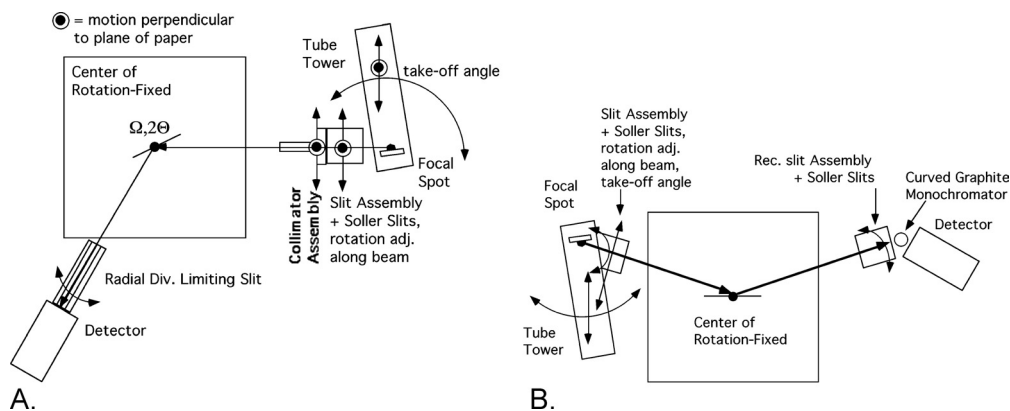


Fig. 8. The functional schematic drawings for the (A) 4-axis (overhead view) and (B) $\theta-\theta$ goniometers (side view) showing relative motions of various parts of the goniometers.

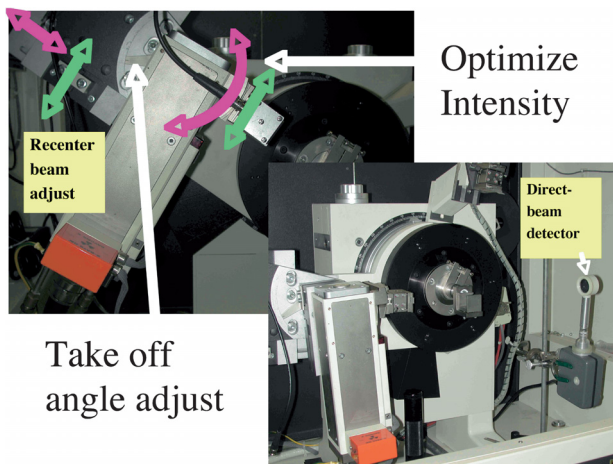


Fig. 9. $\theta-\theta$ unit: Photographs show the locations of the adjustments for setting the take-off angle and aligning incident slit assembly as well as the movements available.

with power level. As always, be aware of the shutter status. Because you will likely need to scan the primary beam, foils to attenuate the beam need to be placed somewhere in the beam path. Copper foils usually work well; the total thickness of the foils should be empirically determined with care so as to not damage the detector. Until one is experienced, gradual increases in power, quick scans and corresponding increases in foil thickness should accomplish this. If applicable, set the energy window on the detector electronics as wide as possible to detect all the X-ray energies emitted from the tube as these contribute to dead time. Once the take-off angle is set and with no sample in place, adjust the mechanisms available (right-most green \Leftrightarrow in Fig. 9) to get the most intense beam possible through the widest slits available. The intensity can be checked either by a direct beam detector or by using the pre-exist-

ing detector with attenuating foils. For the latter, $0^\circ 2\theta$ may have moved substantially necessitating a broad scan range to locate the beam. Next, incrementally insert narrower incident and anti-scatter slit sets, observing the intensity decrease proportionally to reduced angular divergence of the incident slit. Deviations from this proportional reduction likely indicate some misalignment with the incident slit assembly; that is, the beam path is not parallel with the direction of beam travel. The custodian must adjust the position of the slit assembly so as to achieve this proportional reduction in intensity. The tilt on the incident Soller slits should then be optimized with respect to intensity.

The approximate center of rotation of the goniometer must be known or located. Usually the diffractometer comes with either some fiducial surface or a mechanism for placing the sample on the center of rotation of the goniometer (see Fig. A4). The fluorescent screen needs to be mounted such that the fiducial mark on the fluorescing surface is on the center of rotation of the goniometer, and if possible level this surface. A telescope/cathetometer with cross hairs can be very useful here, particularly for the 4-axis unit. The horizontal cross hair can be aligned to the leveled surface of the fluorescent screen at $-90^\circ\chi$ and the vertical cross hair at $0^\circ\chi$. Make sure the sample surface stays on the cross hair as the sample is rotated about the surface normal. The visible fiducial mark on the center of the fluorescent screen must be translated (via XY stages here such that it coincides with the cross hairs of the telescope/cathetometer, which are set on the center of the goniometer. The intersection of the cross hairs is now on the center of rotation, but should be double checked with χ movements to confirm. Alternatively, a laser pointer may be mounted to the

Table III. An alternative method for a θ - 2θ goniometer to experimentally find the center of rotation of the goniometer provided Ω can rotate over 180° .

1. Insert medium wide slits $\sim 1^\circ$ divergence
2. Insert alignment slit into sample mount
3. Scan and detect attenuated beam at $2\theta=0$
4. Rotate glass/alignment slit 180°
5. Repeat: scan and detect attenuated beam
6. Reduce divergence slit size and repeat 1-5
7. If no beam is detected, use burn paper or fluorescent screen to locate beam. Adjust sample slit "height" and tube height accordingly

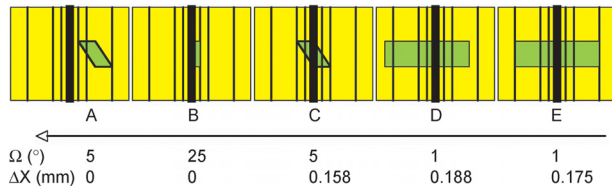


Fig. 10. 4-axis unit: Drawings of the fluoresced images as a function of angle of incidence and incident slit movement perpendicular to beam path. The arrow indicated the direction of the X-ray beam travel.

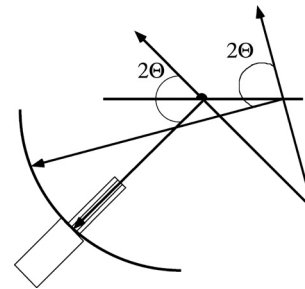


Fig. 11. 4-axis unit: Schematic of initial alignment condition relative to the desired.

detector arm to point at the center of rotation. Iterative adjustments of the sample surface height, the laser spot position and detector arm position are made until the spot no longer moves with detector arm movement (see Fig. A5). Another method for determining the center of rotation is presented in Table III.

The fluorescent screen is a powerful alignment tool in that one can "see" the X-ray beam. Interpretation of the image as a function of angle of incidence provides the key to what adjustments need to be made to obtain a good alignment. We will first consider the 4-axis unit. Figs. 10A and B show that initially the beam was hitting to the right of center and that this effect was reduced as the angle of incidence increased. Further, the slits were rotated about the beam such that the image was of a trapezoid rather than a rectangle. This effect was also reduced as the angle of incidence increased, demonstrating the lack of sensitivity to these effects at higher angular positions. Fig. 11 illustrates this condition showing that the position of the observed diffraction peaks would be lower than the correct positions. In particular, the $\Delta 2\theta$ ($=2\theta_{\text{observed}} - 2\theta_{\text{correct}}$) of low angle peaks would be larger than those at higher 2θ as was observed in Figs. 1 and B1. The slit assembly was moved perpendicular to the X-ray beam in the X/horizontal direction in order to center the image (see Fig. 10C). Fig. 12 shows the adjustments possible to move the slit as-

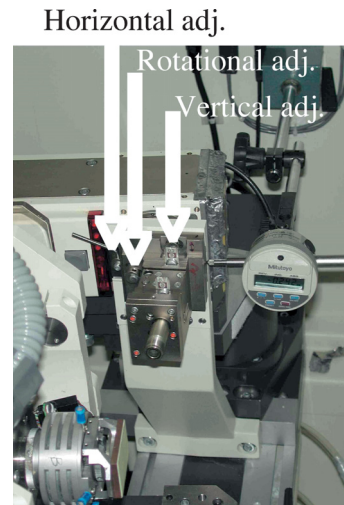


Fig. 12. 4-axis unit: Photograph of the incident slit assembly and the available adjustments to move the slit assembly relative to the X-ray beam. Note: the dial gauge probe to monitor X direction (or other) movements, the 0.2 mm divergence and 0.5 anti-scatter slits bracketing the Soller slits, and the snout/collimator holder where the beam exits.

sembly relative to the X-ray beam. The slit assembly was then rotated to align the slits to the screen transforming the image from a trapezoid to a rectangle. In order to be more sensitive to any misalignments, the angle of incidence was reduced as in Fig. 10D. Because of poor design of the slit assembly, many back and forth movements over $30\ \mu\text{m}$ were required in order to

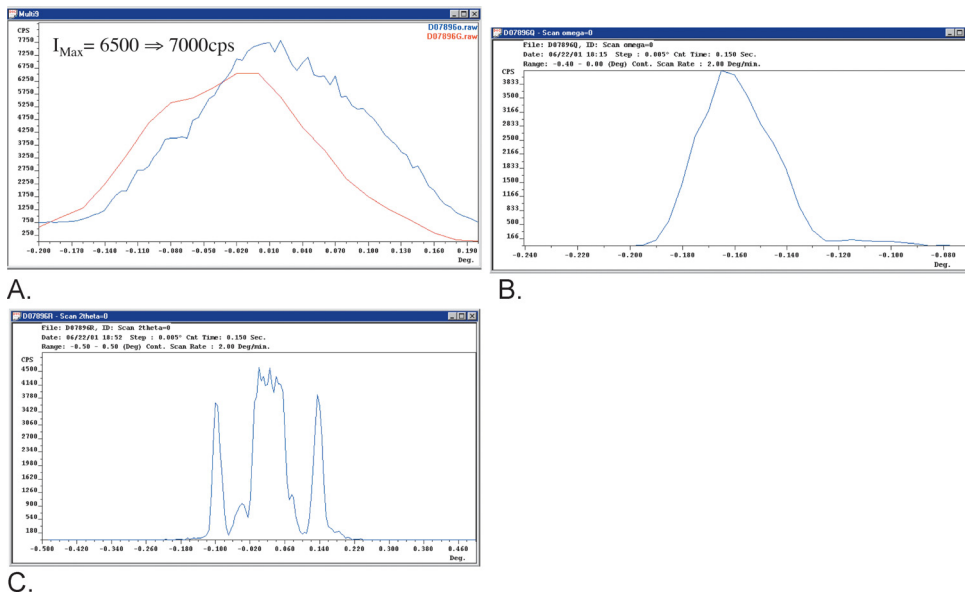


Fig. 13. 4-axis unit: (A) 2θ zero scans with an empty sample position; (B) Ω zero scan with an alignment slit in the sample position; (C) 2θ zero scan with an alignment slit in the sample position.

center the beam at a 1° angle of incidence. Since the vertical placement of the image was good no changes in the vertical/Y direction were needed.

To finish off the “physical” alignment, the fluorescent screen was removed and the sample position was left empty. The detector was scanned to find 2θ zero after Cu foils were inserted on the incident side to attenuate the beam. The acceptance angle of the RDL slits was adjusted to align the long Soller foils parallel to the X-ray beam. This improved the intensity and peak shape (see Fig. 13A). The 2θ zero position was reset physically and electronically. An alignment slit was placed in the sample position with care so that the slit opening was on the center of rotation. In order to find $0^\circ \Omega$, Ω was scanned through zero with the detector at $0^\circ 2\theta$ (see Fig. 13B). The Ω zero position was reset physically and electronically. With the alignment slit and Cu foils still in place and ζ at the new 0° , the detector was rescanned to find 2θ zero. Fig. 13C confirms a good physical alignment showing the primary beam bracketed by two smaller peaks, which are due to reflection of the X-ray beam from the sides of the alignment slit. The intensities of these reflection peaks are effectively equal indicating a well-centered slit around the beam. Any significant difference in intensity between these two reflection peaks indicates some degree of imperfection in the alignment.

Similarly, the fluorescent screen was used on

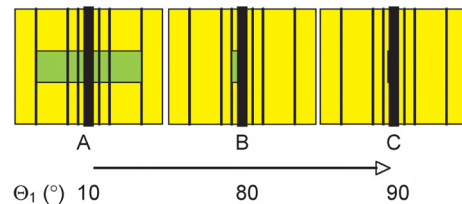


Fig. 14. θ - θ unit: Drawings of the fluoresced images as a function of angle of incidence. The arrow indicated the direction of the X-ray beam travel.

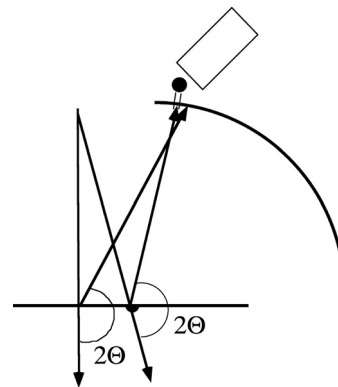


Fig. 15. θ - θ unit: Schematic of initial alignment condition relative to the desired.

the θ - θ unit. Figs. 14A and B show that initially the beam was centered at low 2θ and to the left of center at high 2θ . Fig. 15 illustrates this condition showing that the position of the observed diffraction peaks would be lower than the correct positions. In particular, the positions of the high angle peaks are lower than the correct po-

sitions as was observed in Figs. 2 and B2. Fortunately, we discovered after careful observation that one of the counterweights was miss-set such that the detector arm was missing steps at high 2θ . Thus with no shaft encoder feed-back, the software “thought” the detector was at a higher 2θ than actual, but still low, and recording data as such. The goniometer arm which held the X-ray source was moved to $90^\circ \theta_1$ or angle of incidence, and the tube plus slit assembly was translated (left-most purple and green arrows in Fig. 9) such that the image was centered (see Fig. 14C). The goniometer was then moved back to $10^\circ \theta_1$, and the image was off center. The image was recentered by raising the height of the sample holder (see Fig. A4B), which required adjusting red-painted screws. This adjustment was iterative and not convenient; it required partial disassembly of the sample holder in order to determine the correct screws to turn. In synopsis, Cu foils were inserted to attenuate the beam. The X-ray source and detector were each moved to $0^\circ (= \theta_1 = \theta_2)$, and the detector was then scanned with the tube fixed. A flat plate was then inserted into the sample holder. First the detector was scanned with the tube fixed and vice versa as the plate bisected the beam. This was done iteratively with sample holder adjustment to optimize the intensity, which should be nominally half that from the scan without the plate. If not, one should start with the fluorescent screen to check for what is misaligned. With both angles set at 0° , the flat plate is replaced with the alignment slit, which is rocked iteratively with sample holder screws to maximize the intensity.

This aligns the sample and source with respect to each other. Again, the detector was scanned with the tube fixed and vice versa iteratively in order to optimize the intensity. Once optimized, this defines $0^\circ \theta_1$ and $0^\circ \theta_2$ as well as $0^\circ 2\theta$ and $0^\circ \Omega$ with direct beam detector. The Ω and 2θ zero axis positions were reset physically and electronically.

If everything has been done correctly, the diffractometer is ready to perform the tests outlined in section 4 to further refine the alignment. With the shutter closed, the custodian should remove any attenuating foils and if applicable, narrow the energy window on the detector electronics so as to detect only X-ray energies corresponding to $k\alpha$ lines. This is usually accomplished by scanning an intense peak, such as the (101) quartz with the lower level of the SCA set very low (but above background noise) and the window wide open. After scanning, the custodian should raise the lower level and repeat until 5% of the net intensity has been removed. Next, the custodian should narrow the window and scan again, repeating this until another 5% of the net intensity has been removed. Upon completion, the custodian should rescan and make sure the $k\beta$ has been removed (see Fig. C1).

Diffraction from standard materials is next used to correct 2θ zero errors, perform tilt tests for stress determinations and to check the alignment using the procedures outlined in Appendices B and C. Figs. 16 and 17 each show portions of a LaB_6 diffraction pattern taken on the 4-axis and $\theta-\theta$ units, respectively. When compared to Figs. 1 and 2, respectively, prior to re-

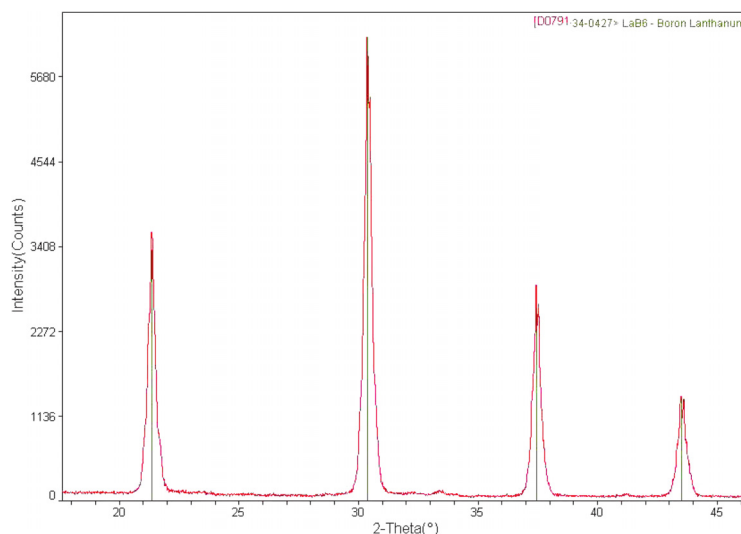


Fig. 16. 4-axis unit: Diffraction pattern of LaB_6 shows peak positions are near PDF card #34-427 values at low 2θ (see full pattern in Fig. B3).

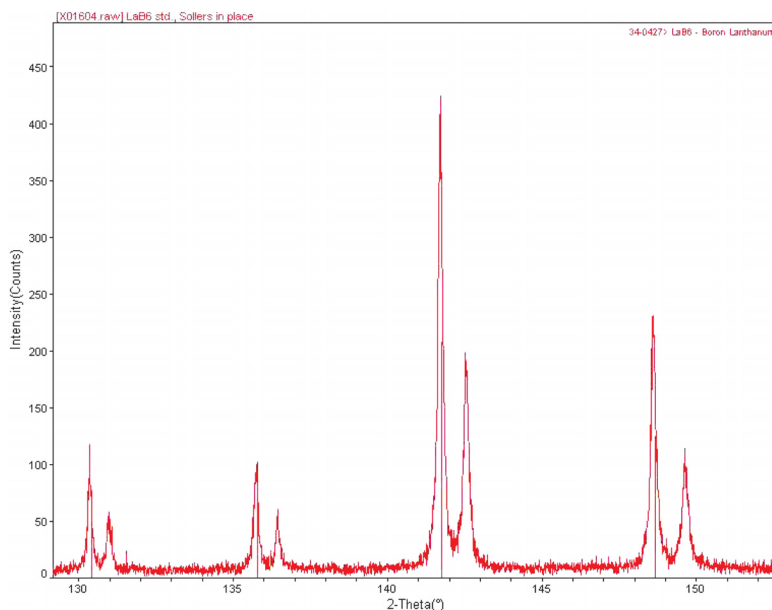


Fig. 17. Θ - Θ unit: Diffraction pattern of LaB_6 shows peak positions are near PDF card #34-427 values at high 2Θ (see full pattern in Fig. B4).

alignment, it can be seen that the alignment of the goniometers has improved the quality of the data considerably. The refined lattice parameters determined from the scans in Figs. B3 and B4 were 4.1566(1) and 4.1569(1) Å for the 4-axis and Θ - Θ units, respectively, which compare favorably to the PDF value of 4.15690 Å [11] (also see Tables BIII and BIV). Neither Tables BIII nor BIV present peaks outside the stated $\Delta 2\Theta$ window of 0.05° as given in Table II. Tables BIII and BIV do reveal 1 and 7 peak positions, respectively, which fall outside the more stringent $\Delta 2\Theta$ window of 0.02° as given in Appendix B for Diffraction angle calibration. The former alignment in this regard was accepted as good. The latter was accepted because only phase ID work was being done at low 2Θ on that instrument. Otherwise another round of re-alignment would be required. When evaluating your alignment, one should consider the primary uses of the instrument. For example when performing stress determinations, absolute peak positions are not as important as relative changes in peak position as a function of sample tilt.

As an aside, the first Θ - 2Θ scan of LaB_6 after re-alignment of the Θ - Θ unit revealed the peak positions were systematically off. This required going back and rescanning with the alignment slit to define 0° Θ_1 and 0° Θ_2 and the location of the fiducial surface corresponding to the center of rotation of the goniometer. The subsequent Θ - 2Θ scan of LaB_6 revealed the peak positions

were systematically offset by a constant 0.04°, which is consistent with 2Θ zero error. The detector arm was moved to the experimentally determined angular value for 8 the (510) LaB_6 . This position was reset physically and electronically to the 2Θ value listed for the (510) LaB_6 on PDF card #34-427, which corrected the 2Θ zero error.

Next, the custodian rechecks the intensity, FWHM/resolution and X-ray wavelength contamination (see Appendix C for details and Fig. C1). Neither W contamination (*viz.* new tube) nor $k\beta$ peaks were observed, indicating that the electronics are set properly on the 4-axis unit for $k\beta$ discrimination. Similar results were also found for the Θ - Θ unit with the maximum intensity of 3670 cps for the (101) quartz peak. The FWHM/resolution decreased somewhat on both units (see Fig. C2). This was not a concern for the 4-axis unit given the choice of optic and the single-phase samples with high symmetry usually examined by this instrument. Although there was 16% reduction in resolution for the Θ - Θ unit, the FOM was close enough to 2 that another re-alignment was not performed.

The tilt tests on the 4-axis unit, critical for residual stress determinations, improved slightly indicating negligible sample surface displacement error and beam misalignment for both χ and ψ tilting in Figs. 18A and B, respectively. Figs. 19A and B show the same when the incident optic is a 1.5 mm diameter pin-hole collimator rather than slits as in Fig. 18. The 0.07°

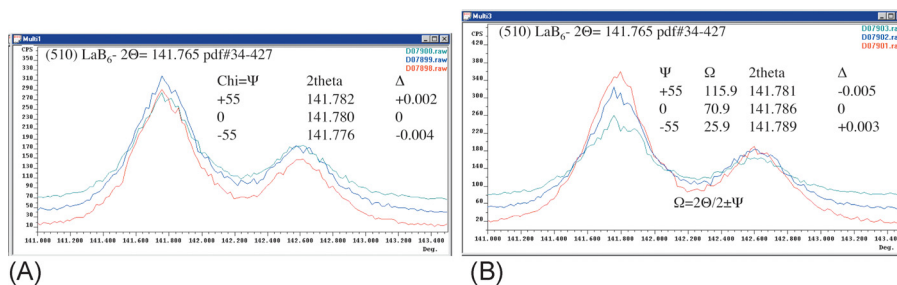


Fig. 18. 4-axis unit: Tilt tests using (A) chi and (B) omega axes showing acceptable alignment.

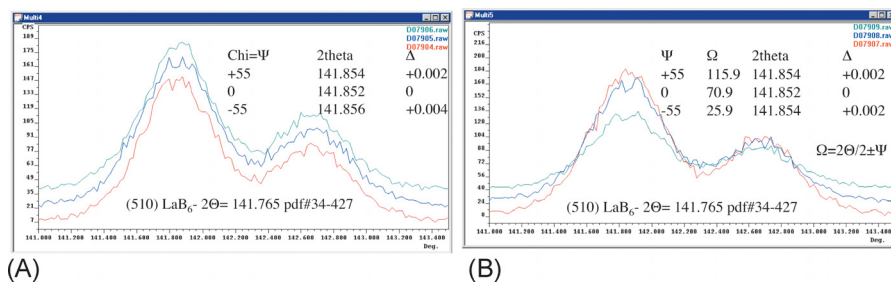


Fig. 19. 4-axis unit: Tilt tests using (A) chi and (B) omega axes showing acceptable alignment using an incident 1.5 mm diameter pin-hole collimator.

2θ change in peak position is due to a small misalignment of the collimator with respect to the focal spot. The 4-axis unit has positioning screws to move the snout (see Fig. 12) independent of the slits. Although not shown, once the alignment appears to be finalized, the authors typically use seven Ψ tilts and apply the criteria in Table II. Often the tilt tests reveal large differences in peak position indicating that the alignment is not good enough. The relative differences can qualitatively tell you what is off and needs to be adjusted. Figs. 20 and 21 provide some guidance in this regard by considering the four most basic situations:

1. the X-ray beam is hitting behind the center of rotation AND the sample surface is located on the center of rotation
2. the X-ray beam is hitting in front of the center of rotation AND the sample surface is located on the center of rotation
3. the X-ray beam is hitting on the center of rotation AND the sample surface is located behind the center of rotation
4. the X-ray beam is hitting on the center of rotation AND the sample surface is located in front of the center of rotation.

The schematics in these figures attempt to illustrate these conditions for Ω and χ tilting, respectively. These figures based on the fact that when the diffracting point on the sample surface is behind the center of rotation the ob-

served peak position (2θ) will be at a lower angle than when the diffracting point on the sample surface is at/on the center of rotation. Likewise, when the diffracting point on the sample surface is in front of the center of rotation the observed peak position (2θ) will be at a higher angle than when the diffracting point on the sample surface is at/on the center of rotation. As is shown, sometimes the sample surface displaced from the center of rotation. The zero tilt condition is the least sensitive to sample surface displacement,¹⁵ due in part to the high 2θ ($>130^\circ$) at which stress determinations are normally done. Since there is usually a small measurable effect of sample surface displacement, the relative peak position is designated as ~ 0 . When two of these condition combine, the qualitative “additions” provide a guide as to the relative peak positions with tilt. Obviously, the use of both positive and negative Ψ tilts is essential to this testing. Based on this, the custodian can determine what to adjust on the goniometer. Of note, Vermeulen provides analytical equations quantitatively modeling the above [13].

Some comments about ASTM E915 are merited as it describes tilt tests with some statistical rigor for alignment verification *only*. Unfortunately, this standard procedure does not require the use of both positive and negative Ψ tilts, which could allow goniometer misalignment

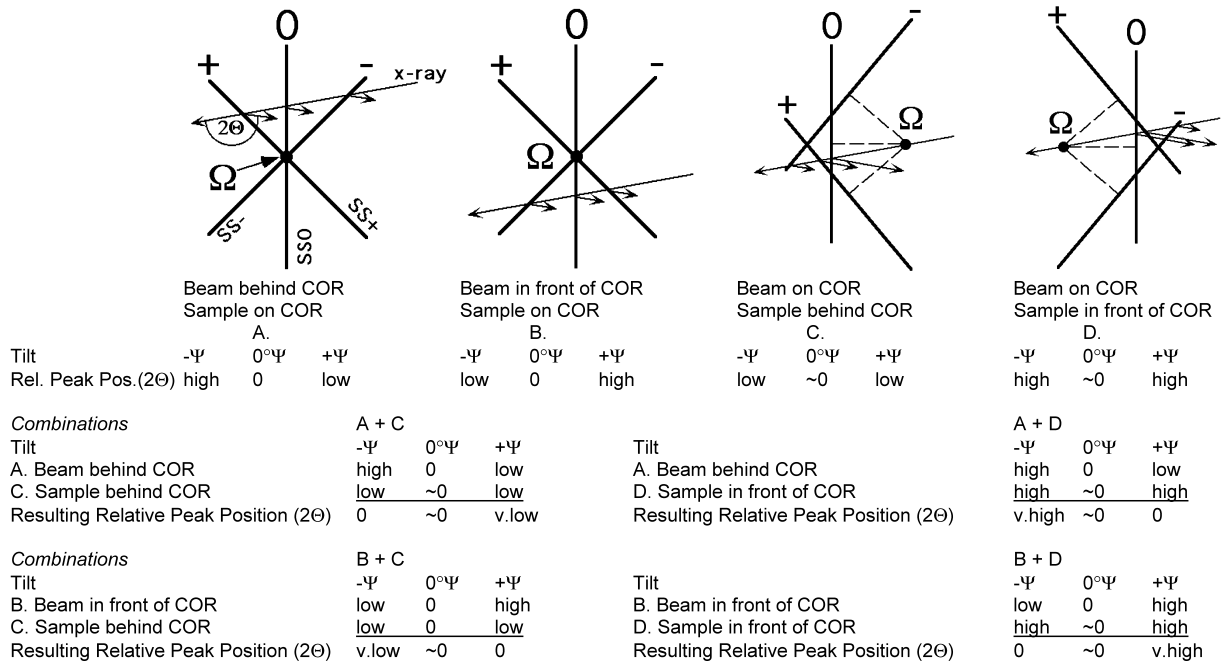


Fig. 20. Schematics to help interpret Ω tilt tests. The peak positions (2θ) are relative to that of $\Psi=0^\circ$. COR= \bullet =center of rotation; diffraction plane is in the plane of the paper; incident beams are going to the left, diffracted to the right; SS $^-$, SS0 and SS $^+$ are the sample surfaces for the negative, zero and positive tilts, respectively. The Ω axis is perpendicular to the plane of the paper and passes through the COR. When in combination, the relative peak positions for the individual conditions can be added to get a qualitative summation.

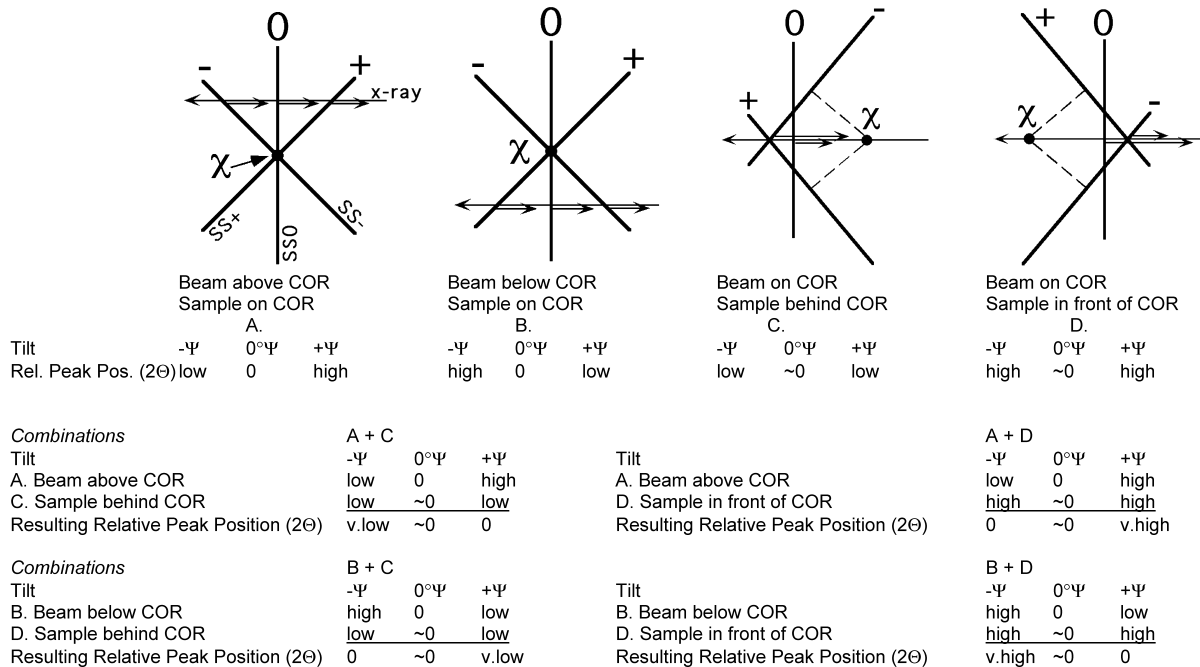


Fig. 21. Schematics to help interpret χ tilt tests. The peak positions (2θ) are relative to that of $\Psi=0^\circ$ tilt condition; COR= \bullet =center of rotation; diffraction plane is perpendicular to the plane of the paper; incident beams are going to the left, diffracted to the right; SS $^-$, SS0 and SS $^+$ are the sample surfaces for the negative, zero and positive tilts, respectively. The χ axis is perpendicular to the plane of the paper and passes through the COR. When in combination, the relative peak positions for the individual conditions can be added to get a qualitative summation.

and/or sample surface displacement to go undetected, resulting in erroneous residual stress values [14]. Another problem with ASTM E915 is that it specifies that correct alignment is accomplished once the average of five stress measurements is 0 ± 14 MPa. As the elastic constant is not specified in the standard, different stress values can possibly be calculated from the same set of strain measurements depending on the elastic constant chosen. Since peak position or interplanar spacing is measured, it is proposed that better criteria would be based on these. Provided the stress free interplanar spacing is reported, crystallographic strain would also be an acceptable alternative. While the practitioner would need to be aware of the changing sensitivity to strain with 2θ , this would allow the flexibility to use other materials/powders instead of just iron powder irradiated with chromium $k\alpha$ X-rays. Since most laboratory X-ray units use copper radiation, which causes fluorescence in iron, this flexibility is needed. However, the fluorescence interference can be dramatically reduced by a diffracted beam monochromator. Within ASTM E915, there is a need to consider the uncertainty associated with the individual measurements. For example, the five individual measurements all have stress values near 0 MPa, but have individual standard deviations greater than 14 MPa. In this instance, while the alignment is correct according to the standard, the authors maintain that there is probably an alignment problem in this situation.

6. How do I maintain the alignment?

Periodic checks every 1 to 8 weeks is a reasonable interval between alignment checks depending upon what you are doing and the amount of usage. Frequently, these checks can lapse and undue effort is expended trying to explain data confounded by an instrument that is out of alignment. Alignment adjustments and alignment check results should be recorded for future comparison and troubleshooting.

7. Standards/Reference Materials for Alignment of Goniometers for Stress Determinations

In order to assure that the X-ray machine is running properly, the custodian must have a set of standards. For powder diffraction, these standards must be polycrystalline, crystallographically random and strain free. As can be inferred from this work, suitable powder standards include Si, LaB_6 and Al_2O_3 . Suitable solid stan-

dards include polycrystalline quartz and Al_2O_3 . These can be obtained from a variety of sources. The necessity of certified standards depends upon your customer base and corporate requirements. Given the expense of certified standards, uncertified standards can be used for most alignments without any compromise. LaB_6 is favored here because of its excellent scattering power due to the high atomic number of La and numerous, intense peaks present over a wide range of 2θ due to its simple cubic structure and relatively large lattice. Alternatively, ASTM E915 procedure describes the preparation of a stress-free iron powder standard [12].

Alignment for stress determinations, particularly the aforementioned tilt tests, single-phase powders with a $10\ \mu\text{m}$ grain size are regarded as ideal. Since powders cannot support long-range stresses, they have zero macro stress. If there were appreciable crystallographic anisotropy or cold work, the peaks would be broadened due to microstresses (micron scale strains) or r.m.s. strains (nano scale strains) and small crystallite size, respectively. Although a material with sharper peaks is preferable, generally speaking, these problems would not preclude using them for alignment. To be clear, these powders do *not* replace the need for a piece/powder of the material that you are studying in order to obtain a stress-free interplanar spacing, d_0 .

Solid samples of known stress values are problematic as testing by numerous laboratories usually produces a wide range of results for the same sample. Still, there is a need/desire for such a standard when equipment or situations warrant. For example, if extensive physical contact is needed to position the sample surface on the center of rotation, a powder would not suffice. One such commercial standard was tested recently.* Iron powder samples were made by gently compressing -325 mesh, 99.9% ferrite powder mixed with a few drops of oil. The resultant disk was glued onto a flat plastic disk. This type sample has a flat, hard surface that is easy to handle. The oil enhances the compaction process and provides some oxidation protection for the sample. LaB_6 powder was mixed with acetone. This slurry was then painted on the surface of the compacted iron disc. Once the acetone evaporated, a thin layer of LaB_6 powder adhered on the surface of the iron disc. Using the same methods as described

* TEC/Materials Testing Division, 10737 Lexington Drive, Knoxville, TN 37932, USA.

Table IV. The stress determinations for a stress-free iron disk, LaB₆ and iron powders.

Sample S#	Stress (MPa)	Strain (ppm)	$\Delta 2\theta$ (°)
LaB ₆ powder alone	29±18	60±27	0.042
04038	1±8	6±23	0.056
04042	0±10	-1±27	0.052
04044	-18±8	-74±22	0.031
04048	-23±8	-93±22	0.057
04048	-23±5	-92±15	0.057
LaB ₆ on disk	-26±26	-52±40	0.013
04044	-20±9	-82±25	0.064
LaB ₆ on disk	34±20	70±30	0.037
04042	-15±8	-59±22	0.077
LaB ₆ on disk	14±21	29±33	0.052
04038	-26±6	-107±17	0.075
LaB ₆ on disk	-21±51	-43±78	0.021
05070	-13±5	-54±12	0.040
LaB ₆ on disk	15±47	30±72	0.055
99.5% Fe powder	-10±3	-39±7	0.060
04042	-18±7	-74±18	0.047
LaB ₆ on disk	74±38	151±59	0.063
04042	-17±12	-69±33	0.092
LaB ₆ on disk	13±30	27±47	0.029
04042*	-5±15	-19±40	0.062
LaB ₆ on disk	1±33	2±51	0.047

$E_{Fe} = 247$ GPa, $\nu = 0.33$; $E_{LaB_6} = 488$ GPa, $\nu = 0.25$; * step size 0.06°

previously (see Table A.I), several iron disks with and without LaB₆ powder painted on were examined. Table IV lists the results in terms of stress, strain and maximum minus minimum peak position. The results from sample #04042 meet the stress-free criteria of ASTM E915 with an average stress of -11 ± 8 MPa. In all cases but one, the strain in the LaB₆ was less than that in the iron disk. Seventeen of the 20 values of $\Delta 2\theta$ were less than twice the guidelines in Table II. The overall average for the commercial iron disk was -15 ± 9 MPa.

8. Summary

Alignment criteria, test procedures and maintenance checks have been described with emphasis on residual strain measurement. The use of standards has also been discussed. Though tersely discussed, important safety considerations were mentioned. It is hoped that this paper will provide insights to safely improve the alignment of instruments to yield more accurate data for the engineering and science communities.

9. Acknowledgements

When performing an alignment, it is often critical to discuss options, scenarios and solutions with others who have a fresh outlook. Thus, this work represents the summation of

numerous conversations with many people. The authors are particularly indebted to Dr.'s Andrew Payzant, Claudia Rawn, Scott Misture, Tom Ely, Xiaojing Zhu, Paul Predecki, Cev Noyan, and Kris Kozaczek for their help and insight. Research sponsored by the Assistant Secretary for Energy Efficiency and Renewable Energy, Office of FreedomCAR and Vehicle Technologies, as part of the High Temperature Materials Laboratory User Program, Oak Ridge National Laboratory, managed by UT-Battelle, LLC, for the U.S. Department of Energy under contract number DE-AC05-00OR22725.

References

- [1] T. R. Watkins, O. B. Cavin, J. Bai and J. A. Chediak: *Advances in X-ray Analysis*, **46** (2003), 119–129.
- [2] R. Jenkins and R. L. Snyder: *Introduction to X-ray Powder Diffractometry*, John Wiley & Sons, Inc., New York (1996), 123, 205–230.
- [3] J. P. Cline and R. W. Cheary: "The Design, Alignment, Calibration and Performance Characteristics of the Conventional Laboratory Diffractometer," Workshop handout, Denver X-ray Conference, 26 July 2000.
- [4] T. R. Watkins and R. D. England: "Workshop W13-Alignment: Maintenance & Alignment Section," Denver X-ray Conference, Steamboat Springs, CO, 31 July 2001.
- [5] T. R. Watkins: "Workshop W8-Diffraction Analysis of Stress and Strain: Practical Application Section," Denver X-ray Conference, Colorado Springs, CO, 2 August 2005.
- [6] H. Krause and A. Haase: "X-ray Diffraction System PTS for Powder, Texture and Stress Analysis," *Experimental Techniques of Texture Analysis*, DGM Informationsgesellschaft Verlag, H. J. Bunge, Editor, (1986), 405–408.
- [7] F. X. Masse, J. Coutu-Reilly, M. Galanek and A. Ducatman: *Health Physics*, **58** (1990) [2] 219.
- [8] C. Weilandics, N. Rohrig, and N. F. Gmur: *Nucl. Inst. Meth. Phys. Res.*, **A266** (1988), 691–698.
- [9] S. Oesch and M. Faller: *Corr. Sci.*, **39** (1997), 1505–1530.
- [10] T. R. Watkins, G. K. Schulze and C. R. Hubbard: ORNL TM to be published.
- [11] Powder Diffraction File, ICDD, Newtown Square, PA 19073–3273 U.S.A.
- [12] ASTM E915-Verifying the Alignment of X-ray Diffraction Instrumentation for Residual Stress Measurement, ASTM, West Conshohocken, PA, 1996.
- [13] A. C. Vermeulen, "Instrument Aberrations in a 4-circle Powder Diffractometer," Accepted to *Zeitschrift fuer Kristallographie*, May 2006.
- [14] E. B. S. Pardue and L. A. Lowery: "Assessment of Component Condition from X-ray Diffraction Data Employing the Sin-Squared-Psi Stress Measurement Technique," *Practical Applications of Residual Stress Technology*, ASM, (1991), 39–46.
- [15] I. C. Noyan and J. B. Cohen: *Residual Stress, Measurement by Diffraction and Interpretation*, Springer-Verlag, New York, (1987), 101–102.